Protein Cell 2013, 4(11): 872–881
DOI 10.1007/s13238-013-3062-5

Protein & Cell

RESEARCH ARTICLE

$CD1d^{hi}CD5^{+}$ B cells differentiate into antibody-secreting cells under the stimulation with calreticulin fragment

Tengteng Zhang*, Yun Xia*, Lijuan Zhang*, Wanrong Bao, Chao Hong✉, Xiao-Ming Gao✉

Soochow University, Institutes of Biology and Medical Sciences, Suzhou 215123, China
✉ Correspondence: xmgao@suda.edu.cn (X.-M. Gao), chaohong@suda.edu.cn (C. Hong)
Received July 16, 2013 Accepted October 11, 2013

ABSTRACT

Calreticulin (CRT) is a multifunctional molecule in both intracellular and extracellular environment. We have previously found that a recombinant CRT fragment (rCRT/39–272) could modulate T cell-mediated immunity in mice via activation and expansion of $CD1d^{hi}CD5^{+}$ B cells as well as induction of CRT-specific regulatory antibodies. Antibody secreting cells (ASCs) are terminally differentiated B cells responsible for producing antibodies to participate in positive immune response as well as immune regulation. In this study, we demonstrate that rCRT/39–272 differentiates murine $CD1d^{hi}CD5^{+}$ B cells into ASCs marked by increased expression of plasma cell-associated transcription factors and production of polyreactive antibodies against DNA and CRT *in vitro*. Intraperitoneal administration of rCRT/39–272 augmented differentiation of $CD1d^{hi}CD5^{+}$ B cells into ASCs in naïve mice or mice with experimental autoimmune encephalomyelitis. Thus, we propose that ASC differentiation and subsequent antibody production of $CD1d^{hi}CD5^{+}$ B cells are key steps in CRT-mediated immunoregulation on inflammatory T cell responses.

KEYWORDS calreticulin, regulatory B cells, antibody secreting cells

INTRODUCTION

Under the stimulation with specific antigens, B cells are activated and functionally matured, thereby exerting immunological functions including antigen presentation and production of multiple cytokines (LeBien and Tedder, 2008; Mauri and Bosma, 2012). Finally, B cells differentiate into antibody secreting cells (ASCs), which are involved in anti-infection immunity and the pathogenesis of immune-related diseases through production of antigen-specific antibodies (Slifka and Ahmed, 1998; Radbruch et al., 2006). It is also evident that ASCs play important roles in negative immune regulation. For instance, $CD138^{+}$ plasma cell-like B cells express IL-10 and exhibit regulatory capability *in vivo* (Neves et al., 2010). Lack of B cells is a main reason responsible for the immunologic disorders in chronic colitis of TCR-$\alpha^{-/-}$ mice (Mizoguchi et al., 1997).

Although calreticulin (CRT) is a major endoplasmic reticulum (ER) residential $Ca2^{+}$-binding and molecule chaperoning protein (Krause and Michalak, 1997; Vassilakos et al., 1998; Arosa et al., 1999; Michalak et al., 1999), soluble CRT can be detected in the serum of patients with autoimmune diseases such as systemic lupus erythematosus (SLE) or rheumatoid arthritis (RA) (Hong et al., 2010; Tarr et al., 2010; Ni et al., 2013). More importantly, recombinant CRT fragments (e.g. rCRT/39–272) possess potent immunostimulatory activities on macrophages (cytokine production) and B cells (Ig secretion and class switching) (Hong et al., 2010). Self-oligomerization is essential for the potent immunological activities of soluble CRT (Jorgensen et al., 2003; Carpio et al., 2013; Huang et al., 2013). Moreover, intraperitoneal (i.p.) administration of rCRT/39–272 modulates T cell-mediated inflammatory responses in mice with experimental autoimmune encephalomyelitis (EAE) via activation/expansion of regulatory $CD1d^{hi}CD5^{+}$ IL-10-secreting B cells (B10 cells) (Hong et al., 2013). Under the stimulation with TLR agonists, B10 cells produce IL-10 which subsequently regulates the balance of Th1/Th2 differentiation both *in vitro* and *in vivo* (Hong et al., 2013). Recently, Maseda et al. reported that regulatory B10 cells could differentiate into ASCs after a transient IL-10-producing stage, and the resultant ASCs contribute to the production of serum polyreactive antibodies (Maseda et al., 2012). Likewise, Madan et al.

*These authors contributed equally to the work.

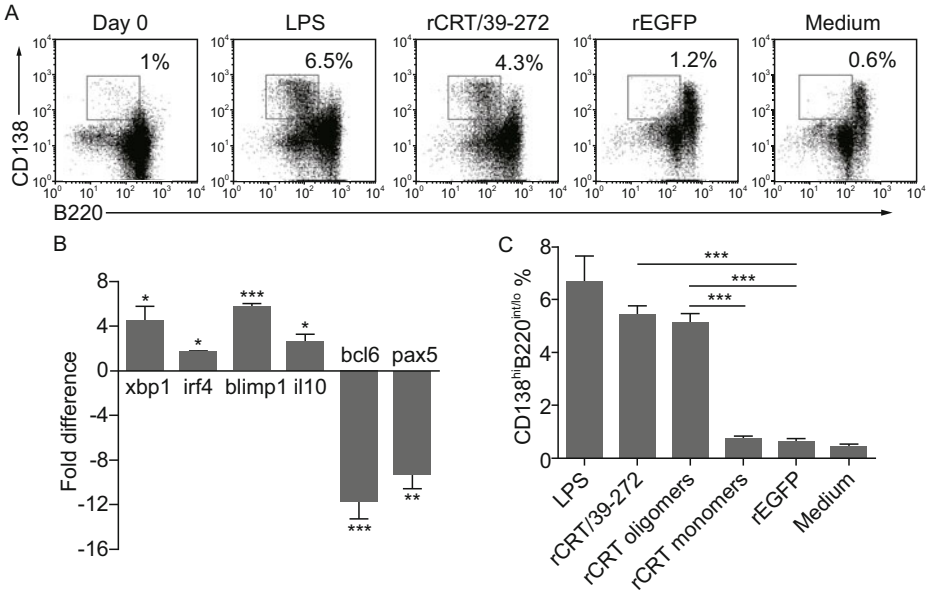

Figure 1. rCRT/39–272 induces B cell differentiation into ASCs *in vitro*. Freshly isolated mouse spleen CD19$^+$ B cells were cultured in the presence, or absence, of rCRT/39–272, rCRT oligomers, rCRT monomers, or rEGFP (30 μg/mL) for 72 h. LPS (1 μg/mL) was also included as positive control. Cells were collected and stained with FITC-labeled B220 and PE-labeled C138 antibodies before flow cytometry analysis (A). Combined results of three independent experiments are also shown in (C). Plasma cell differentiation-associated transcription factor expression in rCRT/39–272-activated B cells was measured by reverse-transcriptase quantitative real-time PCR. Bars indicate mean fold differences between activated and naïve B cells from three experiments (B). *$P < 0.05$, **$P < 0.01$, ***$P < 0.001$.

also demonstrated that LPS-induced IL-10-secreting B cells exhibited phenotypic characteristics of plasma cells (Jeong et al., 2012). Therefore, the present study was designed to address the question whether rCRT/39–272-activated CD1d^{hi}CD5$^+$ cells could make further differentiation into ASCs both *in vitro* and *in vivo*.

RESULTS

Soluble rCRT promotes B cell differentiation into CD138^{hi}B220$^{int/lo}$ ASCs *in vitro*

To address the question if rCRT/39–272 can drive ASC differentiation, mouse splenic B cells were treated with rCRT/39–272, rEGFP, and LPS (as a negative/positive control, respectively) *in vitro*. On day 3, percentage of B cells carrying the ASC surface marker CD138^{hi}B220$^{int/lo}$ (DiLillo et al., 2008) in the rCRT/39–272 group increased from less than 1% to 4.3%, significantly higher than that of the rEGFP group (Fig. 1A). Plasma cell differentiation is known to be associated with the expression of several transcription factors (e.g. *blimp1*, *xbp1*, and *irf4*) and suppression of *pax5* and *bcl6* (Calame et al., 2003). As illustrated in Fig. 1B, expression levels of *xbp1*, *irf4*, and *blimp1* in the rCRT/39–272-treated B cells were approximately 4.5, 1.6, and 5.6 folds higher, respectively, than that of the rEGFP-treated counterparts, whilst the *pax5* and *bcl6* transcripts were markedly reduced in the rCRT/39–272-treated B cells. The *il10* transcript in B cells was also increased significantly in the rCRT/39–272 group, which is consistent with our previous report that rCRT/39–272 drives IL-10 production by B cells *in vitro* (Hong et al., 2013). In line with the essential role of self-oligomerization in rCRT's stimulating effect on macrophages and B cells (Huang et al., 2013), rCRT oligomers exhibited stronger ability in driving B cell differentiation into ASCs than did rCRT monomers (Fig. 1C).

rCRT/39–272 augments the differentiation of ASCs from B1 cells *in vivo*

To evaluate the effect of rCRT/39–272 on ASC differentiation *in vivo*, naïve C57BL/6 mice were i.p. injected with rCRT/39–272 or rEGFP, and sacrificed 3 days later for splenocytes. As shown in Fig. 2A and 2B, percentage of CD138^{hi}B220$^{int/lo}$ ASCs amongst splenic B cells of the rCRT/39–272 group was 3.6-folds higher than that of the rEGFP group (0.97 ± 0.24% vs. 0.27 ± 0.03%), which is in line with the *in vitro* results. Most of the rCRT/39–272-induced ASCs seemed to be derived from B1 cells, as approximately 60% of rCRT/39–272-induced ASCs were CD1d^{hi}CD5$^+$ (B1 cell phenotype), whilst only 6% CD138$^-$B220^{hi} B cells carried the same phenotype (Fig. 2D). 7.44% of CD1d^{hi}CD5$^+$ splenocytes from rCRT/39–272-treated mice carried the ASC phenotype, compared to 1.32% in the rEGFP group (Fig. 2C). These data collectively indicate that rCRT/39–272 effectively induces CD1d^{hi}CD5$^+$ B cells to differentiate into ASCs *in vivo*.

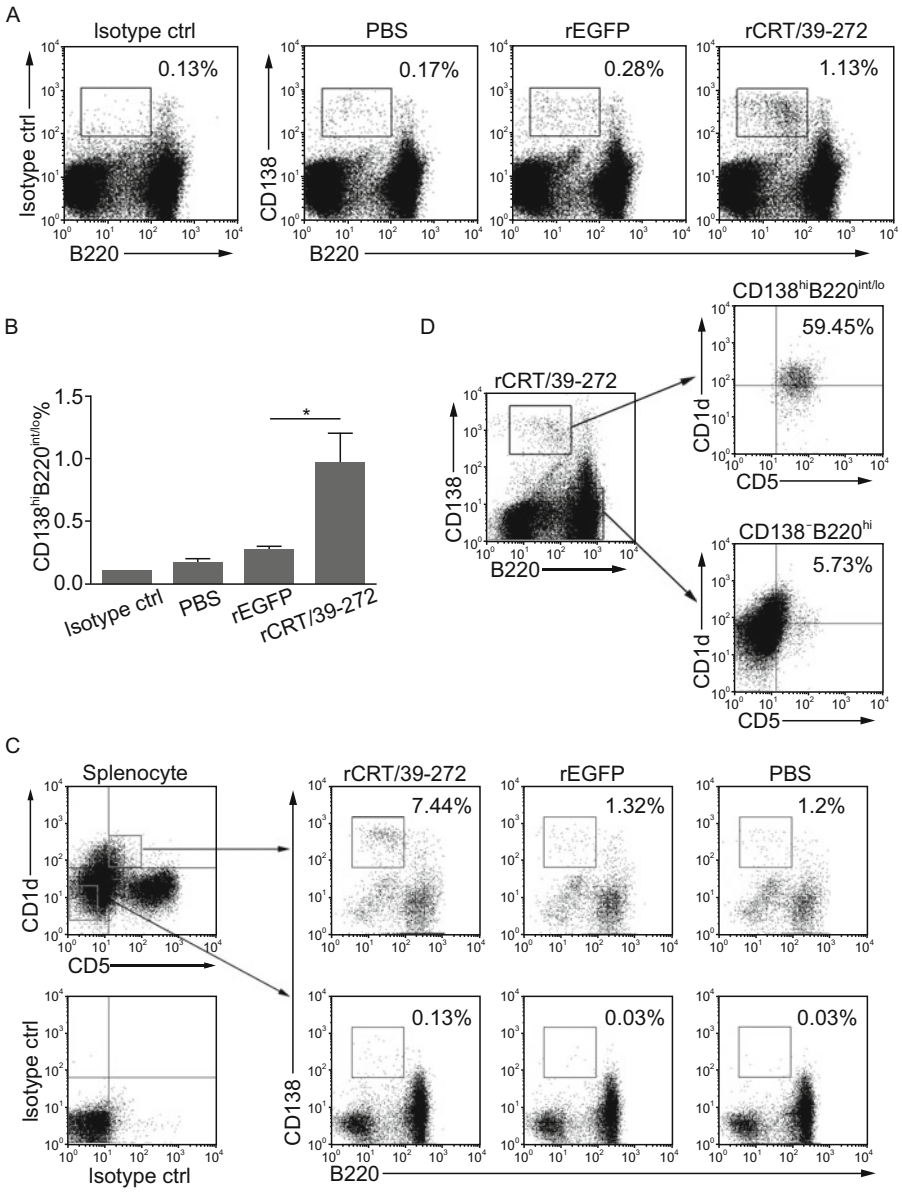

Figure 2. rCRT/39–272 drives splenic B cells to differentiate into ASCs *in vivo*. Naïve C57BL/6 mice (3 mice per group) were i.p. injected with rCRT/39–272 or rEGFP in PBS (100μg/200μL/mouse), or PBS alone, and sacrificed 3 days later for spleens. The collected splenocytes were stained with FITC-labeled antibody against B220, PE-labeled antibody against CD138, or corresponding isotype controls, for flow cytometric analysis (A). 7-AAD solution was added to exclude apoptotic cells. A statistic comparison of percent $CD138^{hi}B220^{int/lo}$ cells in total splenocytes among each group from three independent experiments is shown in (B). $*P < 0.05$. Splenocytes from these animals were also stained with combinations of FITC-labeled B220, PE-labeled CD138, PEcy7- labeled CD5, Alexa Fluor 647-CD1d or isotype control antibodies for FACS analysis on frequencies of $CD138^{hi}B220^{int/lo}$ cells amongst $CD1d^{hi}CD5^{+}$ and $CD1d^{lo}CD5^{-}$ subsets (C). The expression of CD5 and CD1d in $CD138^{hi}B220^{int/lo}$ and $CD138^{-}B220^{hi}$ cells from the rCRT/39–272-treated mice was also analyzed. Three independent experiments were performed and data from one representative experiment are shown in (D).

rCRT/39–272 elicits DNA-specific autoantibody production by B1 cells in mice

$CD1d^{hi}CD5^{+}$ B cells are characterized for the ability to produce polyreactive autoantibodies, some of which exhibit immunoregulatory potentials (Askenase and Tsuji, 2000; Hayakawa and Hardy, 2000; Berland and Wortis, 2002). In the experiment shown in Fig. 3A, freshly fractionated splenic $CD19^{+}$ B cells, $CD1d^{hi}CD5^{+}$ B cells, and non-$CD1d^{hi}CD5^{+}$ B cells were cultured in the presence of rCRT/39–272 or rEGFP for 3 days before the supernatant was collected and analyzed for IgM Abs. After rCRT/39–272 stimulation, $CD1d^{hi}CD5^{+}$, but not non-CD-

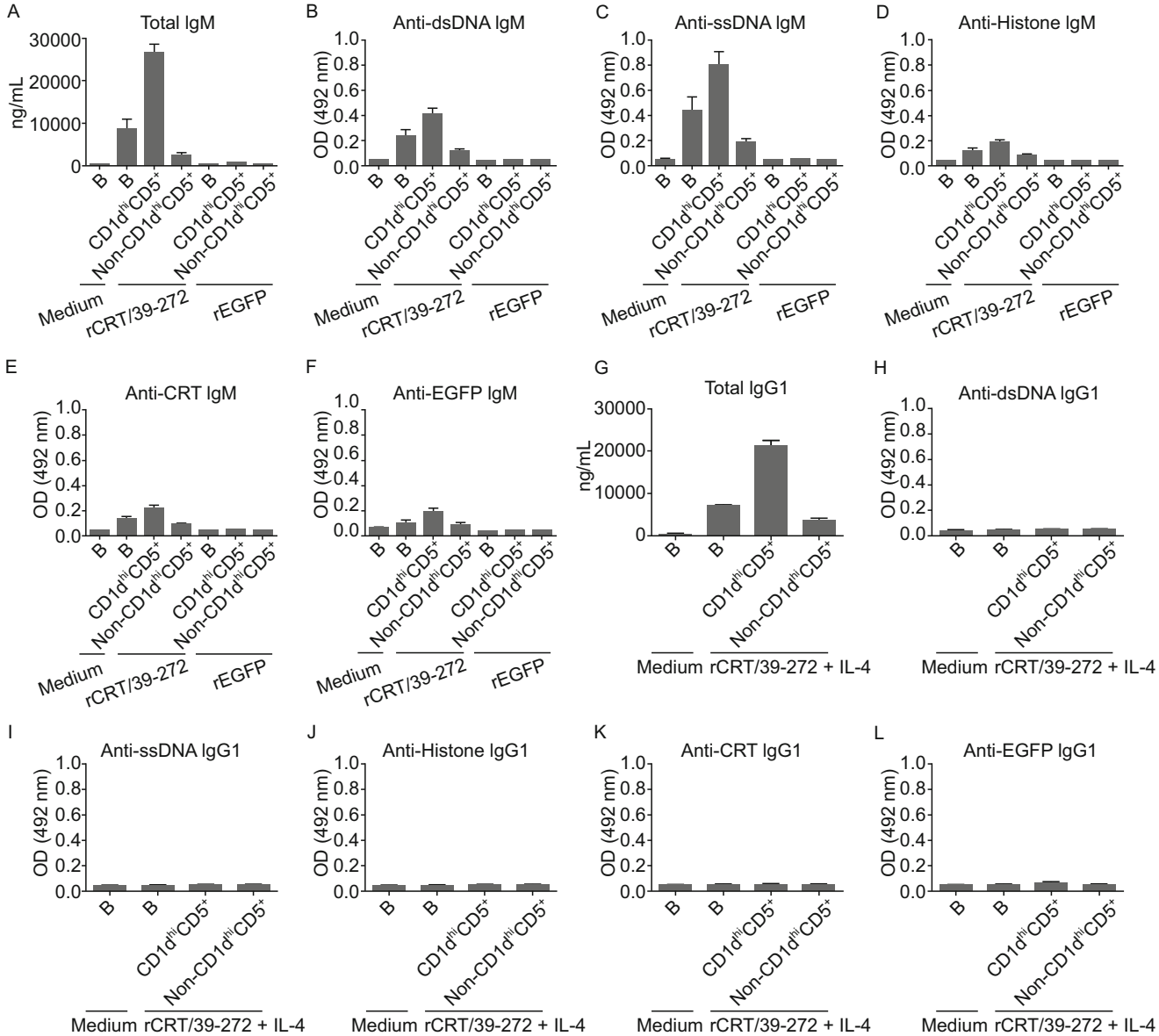

Figure 3. rCRT/39–272 treated CD1d^{hi}CD5^{+} B cells produce anti-DNA antibodies. Freshly isolated splenic CD19^{+} B cells were stained with PerCp-labeled CD5 and Alexa Fluor 647-labeled CD1d antibodies for sorting. The resultant CD19^{+} B cells (B), CD1d^{hi}CD5^{+} and non-CD1d^{hi}CD5^{+} B cell subsets (2 × 10^{5} cells/well) were cultured with 30 μg/mL rCRT/39–272 or rEGFP in the presence/absence of rmIL-4 (20 ng/mL) for 3 days (for IgM) or 6 days (for IgG1) in triplicates in 96-well round bottom plates. CD19^{+} B cells cultured in medium only were included as negative control. Culture supernatants were collected and concentrations of total IgM and IgG1 were measured using mouse IgM and IgG1 quantitative ELISA kits (A and G). Specificity of these Abs was further analyzed using ELISAs based on dsDNA (B and H), ssDNA (C and I), Histone (D and J), rCRT/39–272 (E and K) or rEGFP (F and L). These results represent 3 independent experiments.

1d^{hi}CD5^{+}, B cells secreted substantial amounts of IgM (Fig. 3A). Interestingly, these Abs were able to bind dsDNA and ssDNA, but not histone, rCRT/39–272 or rEGFP, with relatively high affinity in ELISAs (Fig. 3B–F). Next, we cultured mouse splenic CD19^{+} B cells, CD1d^{hi}CD5^{+} B cells, and non-CD1d^{hi}CD5^{+} B cells with rCRT/39–272 plus recombinant mouse IL-4 (rmIL-4) for up to 6 days to induce IgG1 production. As shown in Fig. 3G, IgG1 Abs were produced by the rCRT-activated CD1d^{hi}CD5^{+} B cells. However, these Abs did not recognize DNA, histone, rCRT/39–272 or rEGFP in ELISAs (Fig. 3H–L).

rCRT/39–272 induces B1 cell differentiation into CRT-specific ASCs *in vivo*

It has been illustrated that immunization of mice with rCRT/39–272 elicits CRT-specific Abs capable of modulating T cell

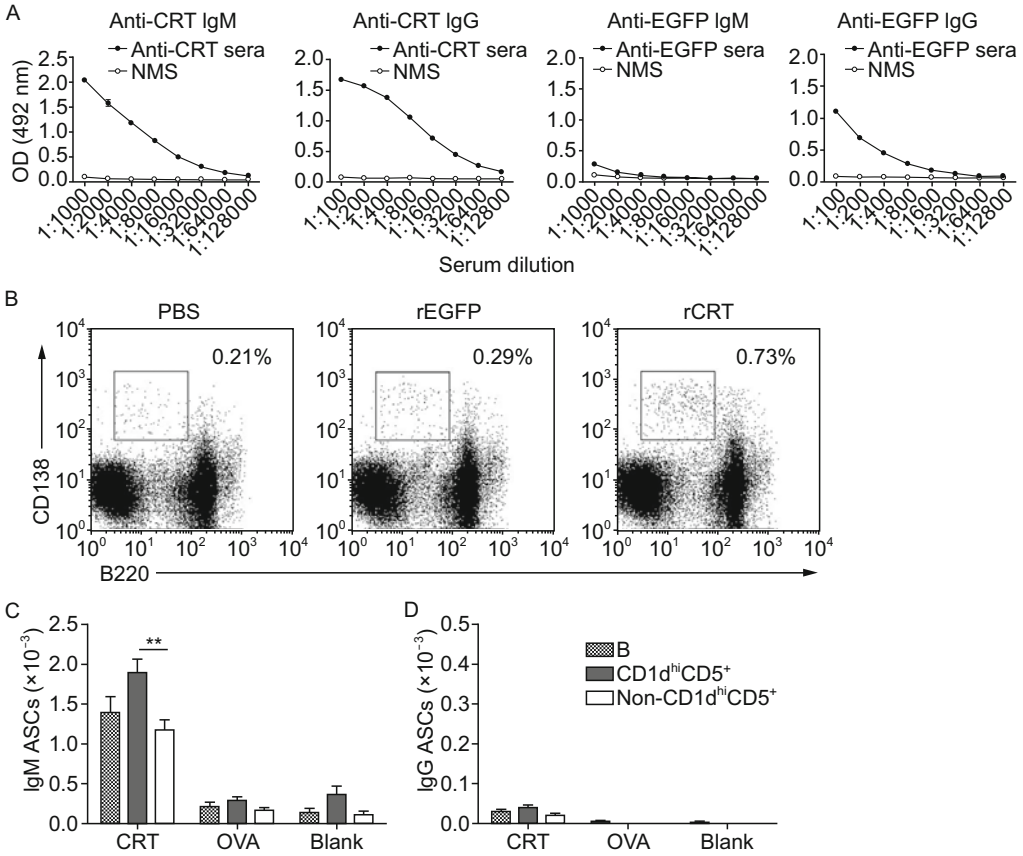

Figure 4. rCRT/39–272 immunization induces CD1d^{hi}CD5^{+} B cell differentiation into CRT-specific ASCs. Naïve C57BL/6 mice were s.c. immunized with 100 μg rCRT/39–272 or rEGFP and boosted twice with half dose of recombinant proteins at a 10-day interval through i.p. injection. Serum samples harvested 10 days after the final immunization were serially titrated against rCRT or rEGFP in ELISAs for detection of CRT- or EGFP-specific IgG and IgM Abs (A). Splenocytes from these mice were stained with FITC-labeled B220 and PE-labeled CD138 antibodies, or isotype control antibodies, for CD138^{hi}B220$^{int/lo}$ cell frequency analysis (B). CD19^{+} B cells, purified using microbeads from the splenocytes of these mice, were further stimulated with 2 μg/mL LPS for 48 h followed by cell sorting into CD1d^{hi}CD5^{+} and non-CD1d^{hi}CD5^{+} B cell subsets, which were cultured on ELISPOT plates (precoated with, or without, rCRT/39–272 or OVA) for 5 h (C) or 48 h (D) to enumerate IgM (C) and IgG (D) secreting cells. Statistic results from three independent experiments are shown. $^{**}P < 0.01$.

responses in DTH and EAE models by interfering its activation and differentiation (Qiu et al., 2012). To further evaluate whether rCRT/39–272 immunization could induce CD1d^{hi}CD5^{+} B cells to differentiate into ASCs capable of producing CRT-specific Abs, naïve C57BL/6 mice were s.c. immunized with rCRT/39–272 or rEGFP dissolved in PBS, or PBS alone, followed by two booster i.p. immunization. Consistent with our previous results (Hong et al., 2010), rCRT/39–272, but not rEGFP, induced strong antigen-specific IgM and IgG responses *in vivo* (Fig. 4A), reflecting the substantial expansion and ASC differentiation of CRT-specific B cell clones after rCRT/39–272 administration. Fig. 4B shows that, 10 days after the final immunization, percentage of the CD138^{hi}B220$^{int/lo}$ cells in the splenocytes of the rCRT/39–272 group was much higher than that of the controls (0.73% vs. 0.29%). Moreover, ELISPOT assays revealed significantly greater numbers of CRT-specific IgM-secreting cells in the CD1d^{hi}CD5^{+} subset than the non-CD1d^{hi}CD5^{+} B cells from these animals (Fig. 4C). It should be noted that the frequency of CRT-specific IgG-secreting ASCs in the rCRT/39–272 group was surprisingly low (Fig. 4D), which seems inconsistent with the higher titer CRT-specific IgG Abs in mice after rCRT/39–272 immunization, shown in Fig. 4A, but can be explained by more superior binding affinity and specificity of the IgG Abs.

rCRT/39–272 induces ASC differentiation in EAE mice

Our previous work showed that i.p. administered rCRT/39–272 inhibits murine EAE severity via activation/expansion of B10 cells *in vivo*, most of which were derived from B1 cells (Hong et al., 2013). It was of interest to determine whether rCRT/39–272 could also drive ASC differentiation in mice with EAE. Naïve C57BL/6 mice were immunized with $MOG_{35–55}$ peptide for EAE induction, followed by i.p. injections of 100 μg rCRT/39–272

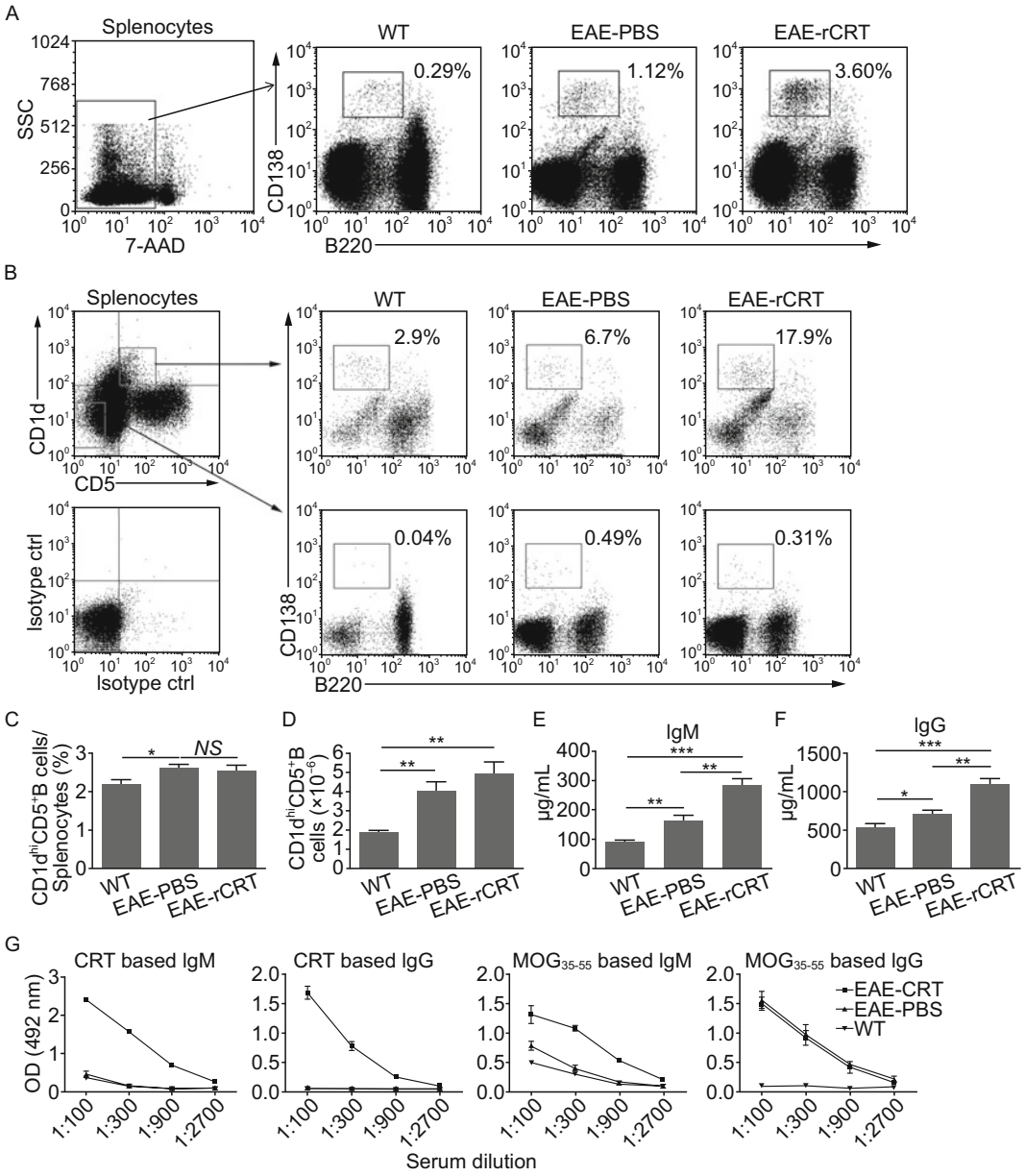

Figure 5. rCRT/39–272 induces CD1d^{hi}CD5^{+} B cells to differentiate into ASCs in EAE mice. Naïve C57BL/6 mice (5 mice per group) were s.c. immunized with 100 μg $MOG_{35–55}$ peptide emulsified in CFA to induce EAE. On day 0 and 2, 100 μg of rCRT/39–272 in 200 μL PBS, or PBS alone, was given to these mice through i.p. injection. On day 9, mice were sacrificed and their splenocytes stained with FITC-labeled anti-B220, PE-labeled anti-CD138, PEcy7-labeled anti-CD5, Alexa Fluor 647-labeled anti-CD1d Abs or corresponding isotype controls. Ratios of CD138^{+}B220$^{int/lo}$/B220^{hi} cells (A), CD138^{+}B220$^{int/lo}$/CD1d^{hi}CD5^{+}, and CD138^{+}B220$^{int/lo}$/CD1d^{lo}CD5^{-}B220^{hi} cells (B) are indicated in the figure. Percentage and absolute numbers of CD1d^{hi}CD5^{+} B cells amongst total splenic B cells are also shown (C and D). Serum samples were collected from the EAE mice, 9 days after induction, for quantitative analysis of IgM and IgG using ELISAs (E and F). Specificity of the serum Abs was confirmed by ELISAs based on rCRT/39–272 and $MOG_{35–55}$ (G). This is a representative of three independent experiments.

at the same day and 2 days later. These mice were sacrificed on day 9 for evaluation of ASC percentage in the periphery. As shown in Fig. 5A, percentage of ASC amongst splenocytes of the rCRT/39–272 group dramatically increased compared to the PBS treated controls. Flow cytometric analysis revealed that such ASCs were predominantly within the CD1d^{hi}CD5^{+} B cell population (Fig. 5B), implying that rCRT/39–272 induced CD1d^{hi}CD5^{+} B cell differentiation into ASCs during EAE progress. As shown in Fig. 5C, although the percentage of CD1d^{hi}CD5^{+} B cells was slightly increased after EAE induction,

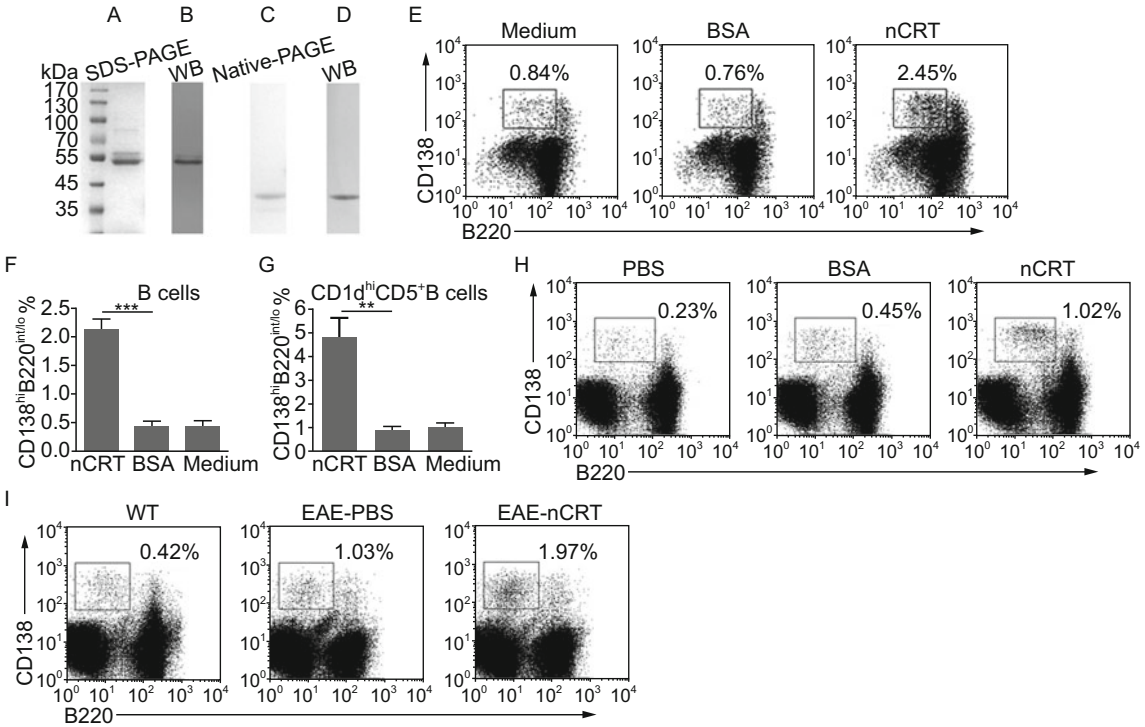

Figure 6. nCRT induces CD1d^{hi}CD5^{+}B cells to differentiate into ASCs *in vitro*. Purified nCRT from mouse livers was run in two identical 12% SDS-PGAE gels (A and B) and two native-PAGE gels (C and D). One of each pair of gels was stained with Coomassie blue (A and C) and the other transferred onto polyvinylidene fluoride membrane for Western blotting with rabbit anti-human CRT Abs followed by visualization with HRP-conjugated goat anti-rabbit IgG (B and D). Freshly isolated splenic CD19^{+} B cells from naïve C57BL/6 mice were cultured in the presence, or absence (Medium), of 30 μg/mL nCRT or BSA for 72 h. Cells were then collected and stained with FITC-labeled anti-B220, PE-labeled anti-CD138, PE cy7-labeled anti-CD5, and Alexa Fluor 647-labeled anti-CD1d Abs for flow cytometric analysis. Frequencies of the CD138^{hi}B220$^{int/lo}$ cells in total splenic B population are shown in (E), accompanied by a statistic analysis of three independent experiments (F). Percentage of CD138^{hi}B220$^{int/lo}$ cells amongst CD1d^{hi}CD5^{+} B cells in each group is also shown (G). $^{**}P < 0.01$, $^{***}P < 0.001$. Naïve C57BL/6 mice (3 mice per group) were given 100 μg nCRT, or 100 μg BSA, in 200 μL PBS or PBS alone through i.p. injection. 3 days later, splenocytes from the treated mice were stained with fluorescence-conjugated Abs. 7-AAD was added to exclude apoptotic cells before flow cytometry analysis. Frequencies of CD138^{hi}B220$^{int/lo}$ cells in the splenic B cell population are shown (H). To analyze the function of nCRT on ASC differentiation in EAE mice, C57BL/6 mice ($n \geqslant 3$ mice in each group) were s.c. immunized with 100 μg $MOG_{35–55}$ peptide emulsified in CFA to induce EAE. On the same day and 2 days later, 100 μg of nCRT or BSA in 200 μL PBS or PBS alone was given to these mice through i.p.. On day 9, mice were sacrificed and splenocytes were stained with fluorescence-conjugated antibodies followed by flow cytometric analysis. Ratio of CD138^{hi}B220$^{int/lo}$/ B220^{hi} B cells is shown in (I).

rCRT/39–272 treatment did not result in a further increase. However, the absolute number of CD1d^{hi}CD5^{+} cells increased significantly in rCRT/39–272-treated EAE mice than that in control mice (Fig. 5D). Concentration of serum antibodies in rCRT/39–272 treated EAE mice was significantly higher than those in parallel groups (Fig. 5E and 5F). Thus, in accordance with the potent immunogenicity and immuno-adjuvanticity of rCRT/39–272, rCRT/39–272 treatment induced the production of both CRT and $MOG_{35–55}$ peptide specific antibodies in EAE mice (Fig. 5G).

nCRT induces CD1d^{hi}CD5^{+} B cells to differentiate into ASCs

To exclude the possibility that rCRT-induced ASC differentiation was a phenomenon specific to prokaryotically expressed rCRT polypeptides, native CRT (nCRT), purified from mouse livers (Fig. 6A–D), was tested for the ability to induce ASC differentiation. As illustrated in Fig. 6E–G, administration of nCRT, but not BSA, in mice induced substantially greater percentage of CD138^{hi}B220$^{int/lo}$ cells amongst total splenic B cells or CD1d^{hi}CD5^{+} cell subset. Moreover, nCRT treatment drives the ASC differentiation in both naïve (Fig. 6H) and EAE mice (Fig. 6I). These data indicate that, similar to rCRT/39–272, soluble nCRT is able to augment CD1d^{hi}CD5^{+} B cell differentiation into ASCs.

DISCUSSION

We have previously shown that i.p. administration of rCRT/39–

272 reduced mouse EAE severity by skewing the balance of Th1/Th2 differentiation, which is attributable to the activation/expansion of regulatory IL-10-secreting CD1d^{hi}CD5^{+} B cells. Herein we further illustrated that rCRT/39–272-activated CD1d^{hi}CD5^{+} B cells can differentiate into ASCs both *in vitro* and *in vivo*. Given that nCRT is also able to enhance the ASC differentiation of CD1d^{hi}CD5^{+} B cells *in vitro* (Fig. 6), our results indicate a novel pathway responsible for the immunoregulation mediated by soluble CRT. This may be of importance as elevation of serum CRT levels is strongly correlated with autoimmune disorders such as RA and SLE in humans (Hong et al., 2010; Tarr et al., 2010). Our recent study revealed that self-oligomerization is a key factor for the extraordinarily potent ability of rCRT to activate macrophages and B cells (Huang et al., 2013). Another line of work in this laboratory has found that, incubation at 42°C or pH5 promotes nCRT oligomerization *in vitro* (He et al., unpublished data), it is thus reasonable to suggest that soluble CRT released at the site of inflammatory responses may self-oligomerize, thereby acquiring potent ability of inducing ASC differentiation. Molecular and cellular mechanisms underlying this phenomenon need further investigation.

The immunoregulatory functions of ASCs have been demonstrated in various mouse models. For instance, B cells (as well as certain autoantibodies that they produce) can play roles as important negative regulators in intestinal inflammation and suppress colitis (Mizoguchi et al., 1997; Genestier et al., 2007). Antibodies specific for certain cell surface molecules can negatively regulate T cell responses by interfering T cell activation and differentiation (Zhang et al., 2003; Qiu et al., 2012). Recently, Neves and coworkers (Neves et al., 2010) have reported that CD138^{+} plasma cell-like B cells could express IL-10 and suppress immunity to *Salmonella* infection through an IL-10-dependent pathway. In our study, treatment of CD1d^{hi}CD5^{+} B cells with rCRT/39–272 *in vitro* led to not only their differentiation into ASCs but also production of DNA-specific autoantibodies (Fig. 3). These data are in agreement with recent work by Maseda et al. showing that regulatory B cells produce germline-encoded nonpathogenic low affinity IgM (Maseda et al. 2012). Since rCRT/39–272 is able to activate/expand regulatory B10 cells that suppress immune responses in an IL-10 dependent manner (Hong et al., 2013), our results may suggest a differentiation pathway from CD1d^{hi}CD5^{+} B cells through a transitional B10 stage to ASCs. However, this hypothesis needs to be confirmed by studies employing IL-10 knockout mice. In any case, rCRT-induced B10 cells and ASCs may collaboratively modulate T cell-mediated inflammatory responses *in vivo*. The roles of rCRT/39–272-induced ASCs in immunoregulation merit further investigation.

MATERIALS AND METHODS

Mice

Female C57BL/6 mice between 6 to 10 weeks were purchased from the Model Animal Research Center (Nanjing, China). All animal experiments were performed according to the guideline for the Care and Use of Laboratory Animals of the Laboratory Animal Ethical Commission of Soochow University.

Proteins

The recombinant murine CRT fragment 39–272 and recombinant EGFP were expressed in *Escherichia coli* (*E. coli*) BL21 and purified using Ni-nitrilotriacetic acid resin (Novagen, Germany) according to the method previously described (Hong et al., 2010). Both recombinant proteins were dialyzed to PBS (pH 7.4), followed by incubation and passing through polymyxin B agarose to deplete possible contaminated LPS.

nCRT was purified from livers of mice using ammonium sulfate precipitation and DEAE ion-exchange column chromatography. In brief, mouse liver cells were lysed with lysis buffer (PBS containing 1% TRITON-X 100 and 1 mmol/L PMSF) after a cycle of freezing at −80°C and thawing, and centrifuge at 18,000 rpm for 15 min to obtain the lysis supernatant. Solid ammonium sulfate was added to the supernatant to reach 50% saturation, followed by another centrifuge at 18,000 rpm for 60 min. The precipitate was discarded and the supernatant was subjected to subsequent fractionation at 85% saturation of ammonium sulfate. After centrifugation at 18,000 rpm for 60 min, the precipitate was dissolved in Tris-HCl buffer (pH 7.4) containing 0.15 mol/L NaCl. The resultant solution was applied to a DEAE ion-exchange column (SephadexA-50, GE Healthcare, Sweden) and eluted with a linear gradient of 0.15–0.5 mol/L NaCl in 20 mmol/L Tris-HCl buffer (pH 7.4). All proteins used in this experiment were at over 90% purity as judged by Commassie brilliant blue-stained SDS-PAGE gels. All protein samples were sterile by passing through 0.22 μm filtration membrane, aliquoted and stored at −80°C until use.

rCRT oligomers and monomers were isolated from rCRT samples according to the method described previously (Huang et al., 2013). Briefly, 5 mL of rCRT samples at a concentration of 10 mg/mL was loaded into a Sephadex G-75 (GE Healthcare, US) column (80 × 2 cm), followed by elution with 0.9% NaCl at 20 mL/h and collected every 2 mL volume. The purity of isolated fractions was judged by running samples onto Native-PAGE gels and stained with Commassie brilliant blue.

EAE induction and recombinant protein injection

Active EAE was induced in 6–10 weeks female C57BL/6 mice according to the method described previously (Hong et al., 2013). Briefly, mice were s.c. immunized with 100 μg myelin oligodendrocyte glycoprotein ($MOG_{35–55}$) peptide (MEVGWYRSPFSRVVHLYRNGK; GL Biochem Ltd., Shanghai, China) emulsified in CFA containing 4 mg/mL heat-killed *Mycobacterium tuberculosis* H37RA (Difco, USA) on day 0. Additionally, mice were received 200 ng pertussis toxin (Sigma, USA) i.p. in 500 μL PBS on day 0 and day 2. To investigate the effect of CRT on ASC differentiation in EAE mice, mice were given 100 μg of rCRT/39–272, nCRT, rEGFP, or BSA in 200 μL PBS through i.p. on day 0 and day 2. 9 days after the EAE induction, mice were sacrificed, ASC frequencies in spleen were analyzed by flow cytometry.

Flow cytometry analysis

Cells were collected and washed with PBS containing 1% BSA (Sigma-Aldrich), and FcRs were blocked using anti-mouse CD16/32

antibodies (BioLegend) for 20 min at room temperature. Subsequently, cells were incubated with FITC-conjugated rat anti-mouse B220 (BioLegend) and PE-conjugated CD138 or isotype controls (BD Bioscience) at 4°C for 30 min. In some experiments, Alexa Fluro 647-conjugated CD1d (BioLegend), PE cy7-conjugated CD5 (eBioscience) or fluorescence-conjugated isotype controls were also included to mark specific B cell subsets. After the staining procedure and thorough washes, 7-AAD was added to exclude apoptotic cells before flow cytometric analysis using fluorescence-activated cell sorter (FACS cantoII; Becton-Dickinson, Rutherford, NJ, USA).

Cell culture and isolation

For purification of murine spleen CD19 positive B cells, mouse spleens were gently disaggregated by pressing with the flat surface of a syringe plunger against a stainless steel sieve (200 mesh). RBCs were lysed by brief treatment with ACK lysis buffer. B cells were enriched by positive selection using CD19-microbeads (Miltenyi Biotec, Germany). The purity of purified B cell population was typically over 95% judged by surface CD19 expression.

For isolation of $CD1d^{hi}CD5^{+}$ and non-$CD1d^{hi}CD5^{+}$ B cells, spleen B cells were cell surface stained with PE cy7-labeled anti-mouse CD5 and Alexa Fluor 647-labeled anti-mouse CD1d antibodies for 30 min on ice. After thorough washes with PBS, $CD1d^{hi}CD5^{+}$ and non-$CD1d^{hi}CD5^{+}$ B cell subsets were sorted using FACS Aria III flow cytometer (BD Bioscience) with purities over 70% and 90%, respectively.

B cells were cultured in complete R10 medium: RPMI-1640 supplemented with 10% (*v/v*) fetal bovine serum (Hyclone, USA), penicillin/streptomycin (100 U/mL), L-glutamine (2 mmol/L) and 2-ME (5×10^{-5} mol/L), in a 5% CO_2 incubator at 37°C, in the presence or absence of LPS (1 μg/mL, Sigma-Aldrich), rCRT/39–272 (30 μg/mL), nCRT (30 μg/mL), rEGFP (30 μg/mL) or BSA (30 μg/mL) (Sigma-Aldrich, cell culture grade) for 72 h before analysis.

Antibody production and specificity analysis

Freshly isolated B cells or sorted $CD1d^{hi}CD5^{+}$ and non-$CD1d^{hi}CD5^{+}$ B cells (2×10^5/well) were stimulated with 30 μg/mL rCRT/39–272, rEGFP in the presence or absence of rmIL-4 for 3 or 6 days. Concentrations of total IgM (3-day) and IgG1 (6-day) in the supernatant were determined using mouse IgM and IgG1 ELISA Quantitation Set (Bethyl Laboratories, Montgomery, TX) according to the manufacturer's instructions. Standard curves were established using mouse IgM and IgG1 and the assay detection limits were 15.6 and 7.8 ng/mL, respectively.

To analyze the antibody specificity, ELISA plates (Nunc, Roskilde, Demark) were coated with rCRT/39–272, rEGFP, Histone (2 μg/mL; Roche, Germany), ssDNA, dsDNA (50 μg/mL; Sigma-Aldrich) in carbonate buffer (pH 9.6) at 4°C overnight. Before dried and coated with dsDNA and ssDNA, the plates were pretreated with protemine (100 μg/mL, Sigma-Aldrich) in water for 1 h at room temperature and then washed 5 times with water. The plate was subsequently incubated with blocking solution (2% BSA in PBS) for 2 h at 37°C. After washes, 100 μL of diluted culture supernatant was added in triplicates followed by incubation for 2 h at 37°C. After further washes with PBS-T, plates were incubated with HRP-labeled goat anti-mouse IgM or IgG1 antibodies (Southern Biotech, USA) for 1 h at 37°C. O-phenylenediamine (OPD) (Sigma) substrate was added (100 μL/well) and the plates were incubated for 2 min at room temperature, followed by the addition of 50 μL 2 mol/L H_2SO_4 per well to terminate the reaction. Optical density (OD) was immediately read at 492 nm using an ELISA plate reader (Bio-Rad Laboratories Inc., Hercules, California, USA).

Real-time PCR

RNA extracted from enriched spleen B cells was used to generate cDNA, with relative transcript levels determined by reverse transcriptase quantitative real-time PCR of triplicate samples. Primers were described as below: for *gapdh*, forward primer 5′-CAAGGTCATCCATGACAACTTTG-3′ and reverse primer 5′-GTCCACCACCCTGTTGCTGTAG-3′; for *il10*, forward primer 5′-GGTTGCCAAGCCTTATCGGA-3′ and reverse primer 5′-ACCTGCTCCACTGCCTTGCT-3′; for *xbp1*, forward primer 5′-AAACAGAGTAGCAGCGCAGACTGC-3′ and reverse primer 5′-TCCTTCTGGGTAGACCTCTGGGAG-3′; for *bcl6*, forward primer 5′-CACACTCGAATTCACTCTG-3′ and reverse primer 5′-TATTGCACCTTGGTGTTGG-3′; for *blimp1*, forward primer 5′-GGAGGATCTGACCCGAAT-3′ and reverse primer 5′-TCCTCAAGACGGTCTGCA-3′; for *irf4*, forward primer 5′-CTCTTCAAGGCTTGGGCATT-3′ and reverse primer 5′-TGCTCCTTTTTTGGCTCCCT-3′; and for *pax5*, forward primer 5′-CAACAAACGCAAGAGGG-3′ and reverse primer 5′-GGGCTCGTCAAGTTGG-3′. Cycle conditions were described as follows: one denaturation step of 94°C for 2 min, followed by 40 cycles of 94°C for 30 s, 60°C for 30 s, and 72°C for 1 min. PCR products were controlled for purity by analysis of their melting curves. Expression threshold values (ΔCt) for each transcript were determined by normalizing to *gapdh* expression within each sample group.

ELISPOT assay

The frequencies of Ab-secreting cells among purified $CD1d^{hi}CD5^{+}$ and non-$CD1d^{hi}CD5^{+}$ B cells were determined using ELISPOT assays. Briefly, splenic $CD19^{+}$ B cells were purified from rCRT/39–272 immunized mice and were cultured with 2 μg/mL LPS for 48 h before cell sorting. Total B cells, sorted $CD1d^{hi}CD5^{+}$ and non-$CD1d^{hi}CD5^{+}$ B cells were added to Immobilon-P Multi-screen 96-well plates (Millipore) that were precoated with rCRT/39–272 (2 μg/mL) at either 10^5 (IgM) or 2×10^5 (IgG) cells/well in complete R10 medium (100 μL). After incubating the plates for 5 h (for IgM) or 24 h (for IgG) at 37°C in a humidified CO_2 incubator, the plates were washed three times and incubated with HRP-conjugated polyclonal goat anti-mouse IgM or IgG Abs (Southern Biotechnology Associates) for 1 h at room temperature. After washing, the plates were colored using TMB substrate (Sigma-Aldrich).

Statistical analysis

All experiments described above were repeated at least three times. Comparison of the data was performed using the Student's *t*-test. Significance was defined as $P < 0.05$.

ACKNOWLEDGEMENTS

This study was supported by grants from PCSIRT (IRT1075), the National Natural Science Foundation of China (Grant Nos. 31370908, 31070781, and 31100633), the National Basic Research Program (973 Program) (No. 2010CB529102), and Foundation of Nature Science of Jiangsu Higher Education Institutions of China (11KJB180011).

ABBREVIATIONS

ASCs, antibody secreting cells; CRT, calreticulin; EAE, experimental autoimmune encephalomyelitis; ER, endoplasmic reticulum; RA, rheumatoid arthritis; SLE, systemic lupus erythematosus

COMPLIANCE WITH ETHICS GUIDELINES

Tengteng Zhang, Yun Xia, Lijuan Zhang, Wanrong Bao, Chao Hong and Xiao-Ming Gao declare that they have no conflict of interest.

All institutional and national guidelines for the care and use of laboratory animals were followed.

REFERENCES

Arosa, F.A., de Jesus, O., Porto, G., Carmo, A.M., and de Sousa, M. (1999). Calreticulin is expressed on the cell surface of activated human peripheral blood T lymphocytes in association with major histocompatibility complex class I molecules. J Biol Chem 274, 16917–16922.

Askenase, P.W., and Tsuji, R.F. (2000). B-1 B cell IgM antibody initiates T cell elicitation of contact sensitivity. Curr Top Microbiol Immunol 252, 171–177.

Berland, R., and Wortis, H.H. (2002). Origins and functions of B-1 cells with notes on the role of CD5. Annu Rev Immunol 20, 253–300.

Calame, K.L., Lin, K.I., and Tunyaplin, C. (2003). Regulatory mechanisms that determine the development and function of plasma cells. Annu Rev Immunol 21, 205–230.

Carpio, M.A., Decca, M.B., Lopez Sambrooks, C., Durand, E.S., Montich, G.G., and Hallak, M.E. (2013). Calreticulin-dimerization induced by post-translational arginylation is critical for stress granules scaffolding. Int J Biochem Cell Biol 45, 1223–1235.

DiLillo, D.J., Hamaguchi, Y., Ueda, Y., Yang, K., Uchida, J., Haas, K.M., Kelsoe, G., and Tedder, T.F. (2008). Maintenance of long-lived plasma cells and serological memory despite mature and memory B cell depletion during CD20 immunotherapy in mice. J Immunol 180, 361–371.

Genestier, L., Taillardet, M., Mondiere, P., Gheit, H., Bella, C., and Defrance, T. (2007). TLR agonists selectively promote terminal plasma cell differentiation of B cell subsets specialized in thymus-independent responses. J Immunol 178, 7779–7786.

Hayakawa, K., and Hardy, R.R. (2000). Development and function of B-1 cells. Curr Opin Immunol 12, 346–353.

Hong, C., Qiu, X., Li, Y., Huang, Q., Zhong, Z., Zhang, Y., Liu, X., Sun, L., Lv, P., and Gao, X.M. (2010). Functional analysis of recombinant calreticulin fragment 39–272: implications for immunobiological activities of calreticulin in health and disease. J Immunol 185, 4561–4569.

Hong, C., Zhang, T., and Gao, X.M. (2013). Recombinant murine calreticulin fragment 39–272 expands CD1dCD5 IL-10-secreting B cells that modulate experimental autoimmune encephalomyelitis in C57BL/6 mice. Mol Immunol 55, 237–246.

Huang, S.H., Zhao, L.X., Hong, C., Duo, C.C., Guo, B.N., Zhang, L.J., Gong, Z., Xiong, S.D., Gong, F.Y., and Gao, X.M. (2013). Self-oligomerization is essential for enhanced immunological activities of soluble recombinant calreticulin. PLoS One 8, e64951.

Jeong, Y.I., Hong, S.H., Cho, S.H., Lee, W.J., and Lee, S.E. (2012). Induction of IL-10-Producing CD1d(high)CD5(+) Regulatory B Cells following Babesia microti-Infection. PLoS One 7, e46553.

Jorgensen, C.S., Ryder, L.R., Steino, A., Hojrup, P., Hansen, J., Beyer, N.H., Heegaard, N.H., and Houen, G. (2003). Dimerization and oligomerization of the chaperone calreticulin. Eur J Biochem 270, 4140–4148.

Krause, K.H., and Michalak, M. (1997). Calreticulin. Cell 88, 439–443.

LeBien, T.W., and Tedder, T.F. (2008). B lymphocytes: how they develop and function. Blood 112, 1570–1580.

Maseda, D., Smith, S.H., DiLillo, D.J., Bryant, J.M., Candando, K.M., Weaver, C.T., and Tedder, T.F. (2012). Regulatory B10 cells differentiate into antibody-secreting cells after transient IL-10 production in vivo. J Immunol 188, 1036–1048.

Mauri, C., and Bosma, A. (2012). Immune Regulatory Function of B Cells. Annu Rev Immunol 30, 221–241.

Michalak, M., Corbett, E.F., Mesaeli, N., Nakamura, K., and Opas, M. (1999). Calreticulin: one protein, one gene, many functions. Biochem J 344 Pt 2, 281–292.

Mizoguchi, A., Mizoguchi, E., Smith, R.N., Preffer, F.I., and Bhan, A.K. (1997). Suppressive role of B cells in chronic colitis of T cell receptor alpha mutant mice. J Exp Med 186, 1749–1756.

Neves, P., Lampropoulou, V., Calderon-Gomez, E., Roch, T., Stervbo, U., Shen, P., Kuhl, A.A., Loddenkemper, C., Haury, M., Nedospasov, S.A., et al. (2010). Signaling via the MyD88 adaptor protein in B cells suppresses protective immunity during Salmonella typhimurium infection. Immunity 33, 777–790.

Ni, M., Wei, W., Wang, Y., Zhang, N., Ding, H., Shen, C., and Zheng, F. (2013). Serum levels of calreticulin in correlation with disease activity in patients with rheumatoid arthritis. J Clin Immunol 33, 947–953.

Qiu, X., Hong, C., Zhong, Z., Li, Y., Zhang, T., Bao, W., Xiong, S., and Gao, X.M. (2012). Modulation of cellular immunity by antibodies against calreticulin. Eur J Immunol 42, 2419–2430.

Radbruch, A., Muehlinghaus, G., Luger, E.O., Inamine, A., Smith, K.G., Dorner, T., and Hiepe, F. (2006). Competence and competition: the challenge of becoming a long-lived plasma cell. Nat Rev Immunol 6, 741–750.

Slifka, M.K., and Ahmed, R. (1998). Long-lived plasma cells: a mechanism for maintaining persistent antibody production. Curr Opin Immunol 10, 252–258.

Tarr, J.M., Winyard, P.G., Ryan, B., Harries, L.W., Haigh, R., Viner, N., and Eggleton, P. (2010). Extracellular calreticulin is present in the joints of patients with rheumatoid arthritis and inhibits FasL (CD95L)-mediated apoptosis of T cells. Arthritis Rheum 62, 2919–2929.

Vassilakos, A., Michalak, M., Lehrman, M.A., and Williams, D.B. (1998). Oligosaccharide binding characteristics of the molecular chaperones calnexin and calreticulin. Biochemistry 37, 3480–3490.

Zhang, X.Y., Liu, X.G., Wang, W., Wang, W.C., and Gao, X.M. (2003). Anti-T-cell humoral and cellular responses in healthy BALB/c mice following immunization with ovalbumin or ovalbumin-specific T cells. Immunology 108, 465–473.